Optimisation of rheological parameters and mechanical properties of Engineered Cementitious Composites (ECC) using regression-based models

Zixuan Tang [a, *], Chrysoula Litina [a], Abir Al-Tabbaa [a]

[a] Department of Engineering, University of Cambridge, Trumpington Street, Cambridge CB2 1PZ, UK

Abstract

Engineered Cementitious Composites (ECC) have superior mechanical and durability performance than conventional concrete. One of the major challenges of producing ECC is to ensure appropriate rheology for uniform fibre distribution, which is the prerequisite of its strain-hardening robustness. In this study, the combined and interactive effects of polycarboxylate-based superplasticisers (SP) and viscosity modifying admixtures (VMA) on the rheological behaviour of ECC was systematically investigated. The evolution trends of yield stress and plastic viscosity were characterised in detail with a rheometer. The most desirable range of rheological condition for uniform fibre distribution was identified and the optimal SP-VMA combinations were predicted by regression modelling. Results showed that ECC produced with the optimised dosages of SP and VMA exhibited 200% enhancement in deflection under four-point bending. This study provides effective guidance on rheology control and optimisation of ECC materials and could further benefit for more extensive ECC development and applications.

Key words:

Engineered Cementitious Composite (ECC), strain-hardening, rheology, regression analysis, yield stress (YS), plastic viscosity (PV), superplasticiser (SP), viscosity modifying admixture (VMA)

[*] Corresponding author. Address: Department of Engineering, University of Cambridge, Trumpington Street, Cambridge CB2 1PZ, UK. Tel: +44 (0) 752 914 3188. E-mail address: zt235@cam.ac.uk

1. Introduction

Engineered Cementitious Composite (ECC), or strain-hardening cementitious composite (SHCC) is a special type of high performance fibre reinforced cementitious composite (HPFRCC) with high ductility [1]. Designed based on micromechanics to optimise the interactions between fibre, matrix and interface, ECC only requires a low volume of fibre reinforcement (typically $\leq$ 2%) to realise efficient fibre bridging [2]. Accordingly, it can achieve comparable strength with standard concrete but more superior tensile strain capacity (> 3%, 300 times of concrete or fibre-reinforced concrete (FRC)) [3]. ECC has much higher energy absorption and fracture resistance capacity than standard FRC due to its strain-hardening and multiple cracking behaviour, having been proved promising for various structural applications [4,5]. ECC can resist aggressive ions due to the controlled tight crack widths (< 100 μm) and could be applied to enhance the durability of traditional reinforced concrete (RC) structures [6,7]. Its intrinsic self-healing ability due to the self-controlled microcracking and the less reactive supplementary cementitious materials (SCMs) as contents has also been emphasized [8,9]. ECC can also be tailored by incorporating other materials (e.g. minerals, polymers, nano-materials) to achieve other superior properties, such as self-cleaning [10], ultra-high strength and ductility [11,12], enhanced or autonomous self-healing [13,14], self-sensing [15] etc. The outstanding performance and flexibility in tailoring and production (e.g. precast, self-consolidating casting, sprayable, extrusion) have made ECC a promising construction material for wide applications [16].

However, one major challenge of producing ECC and other HPFRCC is to ensure consistently optimal mechanical performance for different mix designs and minimise variance [17–20]. The robustness of actual tensile strain capacity of ECC is inherently influenced by fibre distribution and flaw size distribution in the matrix, which has been quantitatively demonstrated by [21–23] by fluorescence microscopy, image analysis and mechanical tests. Non-uniform fibre distribution in the matrix leads to fibre-clumping in some locations while other areas remain fibre-free [24], which could greatly affect the cracking stress, fibre bridging capacity and ductility performance [25]. The issue with uniform dispersion of other additives, e.g. other fibre materials and carbon nanomaterials also widely exists in other composite materials [26–28].

The correlation between fresh rheology and robustness of tensile (or flexural) properties of ECC has also been established and experimentally proved by [22,29,30]. The rheology of ECC mortar (i.e. ECC without fibres) has often been characterised by Bingham model with two parameters, i.e. yield stress (YS) and plastic viscosity (PV) using rheometer or viscometer testing [31]. Results showed both low YS and high PV of fresh ECC mortar are desirable for achieving high tensile strain capacity or deflection capacity; the former is for achieving sufficient flowability for mixing and casting to minimise defects and flaws, and the latter is important for obtaining sufficient shear force to uniformly disperse the fibre bundles and also for ensuring matrix uniformity, stability and preventing segregation. Therefore, rheology control is of great significance for improving matrix properties and fibre distribution to obtain satisfying mechanical performance. Traditionally this has been achieved through 1) changing ingredients and/or mix proportions (especially the water-to-binder ratio (W/B)) to modify cohesiveness and fluidity, or 2) incorporating adequate dosages (or combinations) of chemical admixtures (e.g. superplasticisers (SP), viscosity modifying admixtures (VMA) and air entrainers) to physically modify the rheology without significantly affecting other matrix mechanical properties [32]. Since ECC mix proportions have often been specifically tailored based on micromechanics and the ingredients are often limited by local supplies, the latter method is often preferred due to its much smaller impact to the matrix mechanical properties [29]. Apart from rheology control, specific mixing and user casting skills are also helpful and sometimes necessary to improve or remedy fibre distribution to ensure a high-quality ECC production [33].

Moreover, depending on the different local ingredient properties and specific mix design, satisfying rheology with sufficient PV and low YS is often not easy to achieve simultaneously. In practice, the determination of SP dosage has been more or less an empirical and trial-and-error process. Although some researchers conducted mini-slump (or flow table) tests to check fluidity [34], sufficient viscosity for uniform fibre distribution was still not guaranteed. The main effect of SP is to reduce shear and flow resistance, i.e. to reduce YS by reducing attractive forces between cement particles, leading, however, to a reduction of PV as well [30]. Insufficient PV would not only be detrimental to fibre distribution, but could also cause segregation, bleeding and instability of the mixtures. As studied by [35,36], concrete mixtures with a lower W/B led to a more rapid decrease in YS and PV with the increase of SP dosage (especially for W/B=0.25, which has been commonly applied for ECC design), which implied that SP is prone to overdosage. Therefore, PV, as an important rheological parameter, should also be emphasized during ECC mixing. VMA is an effective admixture for increasing fluid viscosity, enhancing mixture stability and preventing segregation [32,37]. Its potential for aiding fibre dispersion has been proved by [19,22,29,38]. However, both YS and PV of mortar or concrete tended to rise with small dosages of VMA [39], and the overdosage of VMA could potentially result in a non-workable mixture.

As a result, the trade-off effect between SP and VMA make them could potentially work together to achieve optimal rheology with both high PV and low YS at the same time for uniform fibre distribution, but only if their dosage combination is appropriate for the mix design, as also emphasized in [40]. Yet the SP or VMA dosage provided in literature regarding ECC production could not be directly referred to due to several facts. On the one hand, large variations in the rheological nature (flowability, cohesiveness, stability etc.) of fresh ECC mixes could exist due to the different features of local ingredients (e.g. grain size and shape, reactivity) and/or different mix proportions. Specifically, many proportion factors such as sand-to-binder ratio (S/B) and W/B are influential to fresh rheology [29,30], leading to varying difficulty in achieving sufficient PV and low YS at the same time. On the other hand, the reactive contents in locally available commercial SP & VMA can be different, and the recommended dosages specified by producers are only for general cementitious materials. Therefore, in order to develop methods for determining optimum SP and VMA addition that could be generally applied to different mix design, admixture concentration and fibres for ECC, learning the effects of varying dosages of SP-VMA combinations on the rheology of fresh ECC is important. To date, however, testing data available in literature about the effect of SP-VMA combinations on ECC materials are very limited. [38] investigated the effect of a melamine formaldehyde sulfonate (MFS)-type SP combined with a hydroxypropylmethylcellulose (HPMC)-type VMA on the rheology of a PVA-ECC paste. Results showed a generally increasing trend of viscosity with lower MFS or higher HPMC dosages; however, only three combinations were tested, so the detailed trends of rheology with a wider range of MFS-HPMC dosage combinations were unknown. [29] investigated the effect of different factors on the rheology of a high-volume-fly-ash PVA-ECC mortar and analysis of variance (ANOVA) was applied to investigate the individual effects of different variables and their interactions. A polycarboxylate SP and a HPMC-type VMA were studied with six dosage combinations, and results revealed the existence of “saturation points” after which the influence of SP or VMA on rheology turns to the reversed trends. The testing data, however, was still insufficient for precisely describing the rheology patterns. Therefore, the combined and interactive effects of SP and VMA with different dosages on the fresh and hardened properties of ECC is still not well investigated, especially for characterising the detailed trends and patterns of the rheology change. Furthermore, there has been no quantitative method that could be generally applied for determining appropriate dosages of SP-VMA combinations for achieving desired rheology in different ECC materials.

To fill the gaps, the superplasticiser-binder ratio (*SP/B*) and viscosity modifying admixture-binder ratio (*VMA/B*) are considered as two design variables for the control and optimisation

of rheological parameters of ECC. Firstly, the combined and interactive influence of SP and VMA on the YS and PV of ECC were systematically investigated based on 50 different SP-VMA dosages to understand the rheology patterns. Secondly, the rheology trends and patterns were generalised by regression modelling; the contribution and interactions between design variables were quantitatively evaluated through analysis of variance (ANOVA); the optimal SP-VMA dosages for ideal rheological condition for fibre dispersion were further identified. Thirdly, mechanical tests were conducted to confirm the validity of model prediction and a discussion about general guideline for rheology control would be presented. The method and procedure for obtaining ideal solutions of SP-VMA dosages can provide effective guidance on ECC design and rheology control aiming for achieving uniform fibre dispersion, robust ductility and consistent quality, so that trial-and-error methods could be avoided. The study is also essential for the broader application and cost reduction of ECC materials in engineering practice.

2. Experimental procedures

2.1. Materials & mix proportions

CEM-I 52.5N high strength Portland cement (PC) (BS EN 197-1) (supplied by Hanson, UK) was used. The cement was passed through the 850-μm sieve before use to ensure consistency. Graded silica sand (S) (supplied by Minerals Marketing, Redhill, Surrey) with a maximum grain size of 250 μm and average grain size of around 110 μm was used as fine aggregate (Fig. 1). Low-calcium fly ash (FA) with fineness category N (featuring coarser particle sizes than category S according to BS EN 450-1, supplied by CEMEX, UK) was applied as a supplementary cementitious material. The physical and chemical properties of the solid ingredients are given in Table 1. 12-mm polyvinyl alcohol (PVA) fibres (produced by Kuraray, Japan) were used, which were coated with oil to reduce interfacial chemical bonding and improve the strain-hardening effects of ECC. Comparing with shorter PVA fibres (e.g. 8 mm), 12-mm fibres have greater potential for developing ECC with high ductility and tensile strength or low fibre volume, but the longer fibres could be more difficult to disperse with a higher tendency of balling and clotting during mixing, leading to a higher demand for precise rheology control. The properties of PVA fibres are given in Table 2. Two chemical admixtures supplied by Sika UK, a polycarboxylate-based SP and a carbohydrate complex-based VMA together with tap water (W) were used to control and adjust rheology of ECC. Before the study, three different types of polycarboxylate-based SPs were preliminarily tested combined with VMA, and similar trends of rheology change were observed despite different efficiency or absorbing rate. Therefore, only one type of SP combined with VMA was applied in this study to reduce the number of variables and mainly focus on the effect of different dosage combinations. The mix proportions for all the tests in this study are provided in Table 3. A high FA content with FA/PC=2.8 was applied (named as F28-ECC in this study). Compared with the "standard" ECC with a fly ash-to-cement ratio of 1.2 (M45-ECC), high-volume-fly-ash ECC (HVFA-ECC) (with a typical fly ash to cement ratio $\geq$ 2.2) has shown multiple benefits e.g. reduced cement consumption and carbon footprint, reduced crack width and higher durability (better freezing-thawing resistance, reduced ion penetration, lower water permeability, etc.), long-term strength development, lower hydration heat, reduced shrinkage and creep, reduced strain rate sensitivity, improved autogenous healing capacity [29,41–45] and worth investigating. Although higher volume of fly ash could help improve mixture flowability due to its fine sphere-shaped particles [41,46], fly ash could also reduce plastic viscosity of the mixture, as supported by both existing literature [47] and our own preliminary tests (Fig. 2), which is unfavourable for sufficient fibre dispersion and mixture cohesiveness. In this case, VMA could be helpful for improving the rheological conditions. W/B and S/B were kept constant at 0.26 and 0.36 respectively as specified by micromechanical design. The PVA fibre volume fraction was kept at 2%. *SP/B* and *VMA/B* were varied based on a factorial design in rheology tests to set up different combinations.

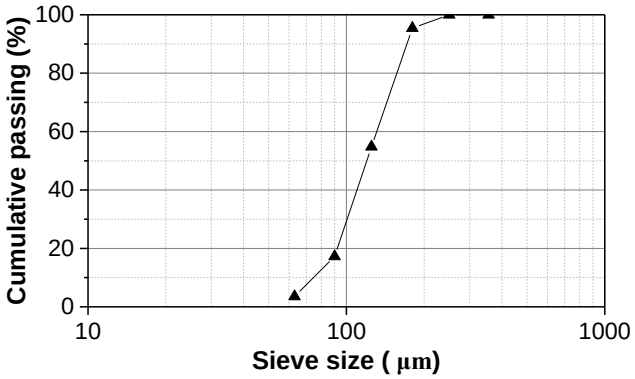

Fig. 1. Typical particle size distribution of the silica sand.

Table 1. Chemical compositions and physical properties of the cement, sand and fly ash used.

Chemical composition, %	CEM I 52.5N	Silica sand	Fly ash (monthly average)
CaO	64.2		Reactive 4.01 (free 0.55)
SiO_2	19.6	98.8 (98.30 Min)	48.5
Al_2O_3	4.8	0.21 (0.25 Max)	24.9
Fe_2O_3	2.7	0.09 (0.16 Max)	9.5
SiO_2+Al_2O_3+Fe_2O_3	27.1	99.1	83.29
MgO	1.2		1.54
SO_3	3.2		0.74
K_2O		0.03	2.9
Na_2O			1
Total alkalis as equivalent Na_2O			2.73
Cl			0.01
Loss on ignition (%)	2.1	0.14	5.25 (Category B)
Physical properties			
Specific gravity	2.75-3.20		2.28
Surface area (m^2/g)	0.30-0.40		
Fineness			23.6 (Category N)
Bulk density (kg/m^3)	900-1500	1350 (loose)	800-1000
Particle size (μm)	5.00-30.00	Maximum 250	< PC
Grain shape		Angular	Sphere

Table 2. Properties of PVA fibres.

Density (g/cm^3)	Tensile strength (GPa)	Elastic modulus (GPa)	Elongation (%)	Diameter (μm)	Length (mm)	Melting point (°C)	Surface oil coating (%)
1.3	1.56	41	6.5	40	12	230	1.2

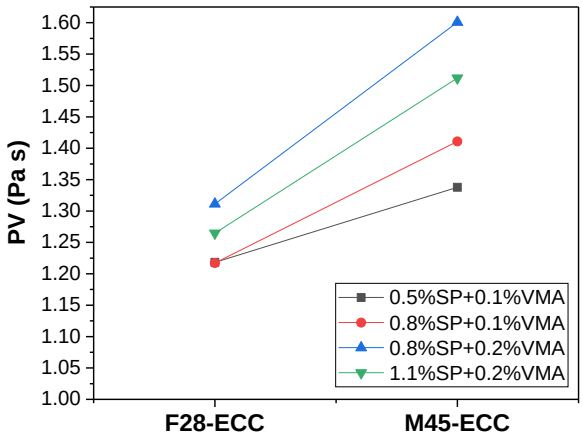

Fig. 2. Comparison of plastic viscosity of different ECC mortar. F28-ECC mortar tended to result in lower viscosity than M45-ECC, which was unfavourable for fibre distribution.

Table 3. Mix proportions of the ECC applied in this study.

Ingredients	PC	FA	S	W	Fibre	*SP/B*	*VMA/B*	W/B	S/B
Mass ratio	1	2.8	1.4	1	2 vol%	0.20 –	0.10 –		
Unit weight (kg/m3)	300	842	416	300	26	1.30 %	0.40 %	0.26	0.36

2.2. Batch mixing, specimen casting and curing condition

A 20-L three-speed Hobart mixer (A200N) including a stainless-steel bowl and a planetary mixing blade was used for batch mixing. Cement, sand and fly ash were first dry mixed with low speed for 2 min. Then the pre-mixed solution containing SP and VMA was added with low mixing speed within 1 min. Then the mortar was mixed at medium speed for 2.5 min for SP to be gradually absorbed in the mix and fully take effect until uniform. After that, a flow table test performed to evaluate the fluidity of fresh ECC mortar (i.e. without fibres) according to BS EN 12350-5 [48]. [22,29] have demonstrated that the flow spread has a high correlation with YS. In this study, a truncated cone (top diameter: 40mm, bottom diameter: 100mm) was used and no tamping or table drop was applied since the ECC mortar was highly flowable (Fig. 3). The flow diameter is defined as the average of the maximum diameter of the spread mortar and the perpendicular diameter. The process took around 10 minutes. At last, fibres were added with low mixing speed in 1 min and mixed with medium speed for another 3 min.

Fig. 3. Flow table testing setup and ECC flow spread.

The fresh ECC mixture was then cast into moulds; light rod tamping and manual pressing on edges was conducted to eliminate large air pores inside. No vibration was required as the mixture was self-levelling. The mixing and casting details were kept as consistent as possible for each batch. After casting, the specimens were covered with plastic sheets for 48 hours and then demoulded. The specimens were cured in ambient environment with 50 ± 10% RH and a temperature of 23 ± 2°C.

2.3. Testing methods

2.3.1. Rheology tests

The rheological properties of fresh ECC mortar (without fibres) were tested by Brookfield DV3T rheometer with a rotatable spindle in the centre of a sample container (Fig. 4a). This is to investigate the combined effect of SP and VMA, and further to determine the appropriate dosages of SP and VMA for ECC production. Based on factorial design and preliminary trial tests, and also referring to recommended dosages provided by supplier and generally applied in literature, *SP/B* was varied from 0.20% to 1.30% (0.10% increment) and *VMA/B* ranged between 0.10% and 0.40% (0.05% increment) to form different combinations to systematically investigate the trends of YS and PV. Duplicate or triplicate tests were conducted. Combinations leading to rheological values out of the machine range or tests with low fit of confidence (< 90%) were discarded.

For each test, ingredients were first dry mixed thoroughly and then SP-VMA solution was added, followed by alternative medium-speed hand mixing and high-speed vortex mixing until the mix was uniform without any solid particles and smoothly flowable. Then the sample was poured in the rheometer container (about 5 mL) for the pre-defined shear protocol to start. Considering the time and temperature effect of SP and VMA, the starting time of each rheology test after wet mixing was controlled as the same time when fibres were added in large batch mixing. The testing temperature was also controlled at 23±2 ℃ by maintaining central air conditioning in the laboratory to minimise testing variability.

Different shear protocols (including range of shear rates, shearing duration for each step, temperature, etc.) would result in different responses or parameter results, so the protocol was kept consistent for testing different mixtures. The range and steps of shear rates in this study were adopted from [29,30] and correspond to real mixing conditions for concrete applications. After the effect of stress history had been eliminated by maximum speed shear, the rotation rate N increased from 0 to 120 rpm step by step (corresponding to the shear rate 0 – 40.8 /s) and then reduced to zero (20 s duration for each step), as shown in Fig. 4b, to generate different resistant torques T corresponding to different shear stress. After the pre-designed shear protocol was finished and with automatic unit transformation, the shear stress τ (Pa) – shear rate $\dot{\gamma}$ (s^{-1}) graph could be obtained. Results were interpreted by Bingham model (Eq. 1), where the PV (μ) is defined as the slope of the descending leg in the graph, and the YS (τ_0) is the intercept of the shear stress axis.

$$\tau = \tau_0 + \mu\dot{\gamma} \quad \text{Eq. 1}$$

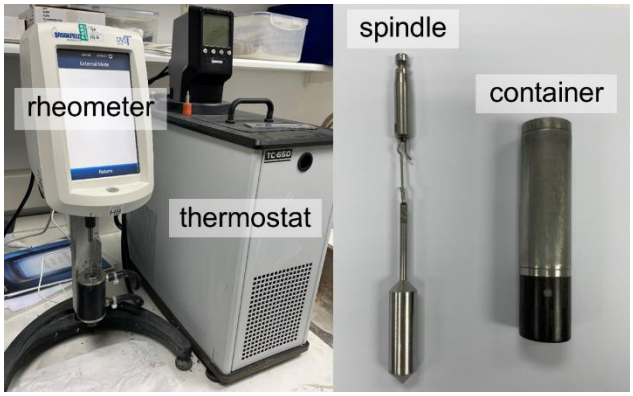

(a)

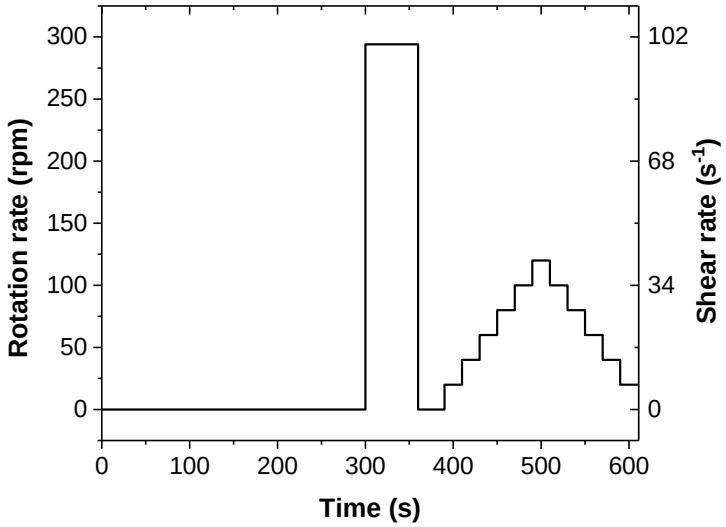

(b)

Fig. 4. The rheometer set up used in the experiments (a) the rheometer, temperature controller and spindle and (b) the shearing profile used for the rheology tests.

2.3.2. Mechanical tests for hardened properties

To verify the influence of fresh rheology on the mechanical characteristics of hardened ECC, four-point flexural tests were conducted on 28-d ECC specimens to assess the deflection capacity (Fig. 5). Previous studies have shown that the deflection capacity can be directly related to the tensile performance of ECC [49,50]. The tests were adapted from ASTM C1609 for fibre-reinforced concrete beams using a third-point loading method [51]. ECC prisms with a dimension of 300 (length)×50 (width)×26 (height) mm^3 were tested under displacement control with a quasi-static loading rate of 0.5 mm/min. The loading span was 80 mm and the supporting span was 240 mm. The midspan deflection (v) of each specimen was monitored and recorded by a laser extensometer.

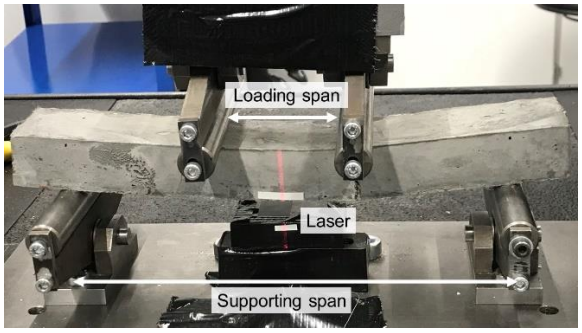

Fig. 5. The setup for four-point flexural tests with a loading span of 80 mm and a supporting span of 240 mm.

Compressive strength tests were conducted on hardened specimens aged 3 and 7 days to study the effect on SP and VMA on early-age strength development. Cubic specimens (40×40×40 mm^3) were tested with a vertical loading speed of 2400 N/s according to BS EN 196-1 [52].

2.3.3. Isothermal calorimetry

Isothermal calorimeter (Calmetrix I-CAL 2000 HPC) was used to test the hydration rate and heat of hydration of fresh ECC mortar based on BS EN 196-11. It was to investigate the effects of SP-VMA dosages on the initial hydration process of ECC, and also to estimate the initial setting time. The heat flow generated by a fresh sample at constant temperature of 23 ℃ was monitored for about 100 hours. The heat of hydration was characterised by the thermal power produced per unit weight of cementitious materials (or binder, PC + FA) in the mixes. The initial setting time was defined as the time at one-third of the peak power. Cumulative energy released were also obtained.

3. Results & Discussion

3.1. Rheology patterns

In the rheology tests, the shear rate $\dot{\gamma}$ and shear stress τ showed a linear relationship and could fit the Bingham model. YS and PV could be obtained from each shear stress-rate plot as the intercept and the slope of linear regression of the downward results to avoid the effect of shear history. The confidence of fit for all the testing results was above 99%, below which a few tests were discarded. 50 SP-VMA combinations were tested and analysed. Fig. 6 and Fig. 7 show YS and PV with increase of SP/B for different VMA dosages, respectively. Each data point represented the average result of two effective tests (i.e. results with tolerable deviation) and outliers were discarded.

3.1.1. Trends of YS with SP-VMA combinations

As shown in Fig. 6a, when SP increased without incorporating VMA, YS was initially as high as 2.8 Pa (representing a stiff and hardly workable mix), then rapidly dropped to the negative-value area. It should be noted that negative YS represented a deviation from Bingham model, indicating the loss of inter-particle cohesion after high-rate shearing, namely segregation of the mixture, as also observed by [30]. The segregation dosage of SP without VMA for this mixture was about 0.45%. After incorporating VMA (dosage $\geq$ 0.10%), however, YS exhibited different patterns, i.e. with increasing SP dosage, YS first decreased to a minimum value and rose again (barely going below zero), showing that VMA could effectively stabilise the mixture and prevent segregation. Increasing VMA was also more effective in increasing YS under high dosage of SP (e.g. $\geq$ 0.70%).

With increasing dosages of VMA until 0.25%, YS generally increased for all SP dosages investigated, and the minimum YS that could be achieved became higher (Fig. 6b). When the minimum YS for a specific VMA dosage was too high for satisfying mixing and casting regardless of the SP dosage, overdosage of VMA was apparent. On the other hand, it could be inferred that with insufficient VMA (possibly between 0% and 0.10% based on testing results), YS could still turn negative with overdosed SP, meaning the stabilising effect was not strong enough and the mixture would still be subject to segregation. Therefore, the VMA dosage should be determined reasonably between the two limits. An ideal combination of SP and VMA should lead to a low but positive YS to maintain high flowability of the mixture but also avoid segregation.

As also described in [29,40,53], the effect of SP and VMA on YS and PV tended to show inverse trends or become less effective on rheology after exceeding the "saturation dosages (or saturation points)". The saturation dosage of SP tended to fluctuate at 0.70% in this study regardless of VMA dosages, but the increase of YS with increasing SP/B after the SP saturation dosage became more rapid when VMA/B was high (Fig. 6a), revealing the interactive effect between SP and VMA. YS decreased for nearly all the SP dosages when VMA/B was over 0.25%, exhibiting an inverse trend, which indicates that the saturation dosage of VMA could be around 0.25% (Fig. 6b). The saturation dosages for both SP and VMA seemed to be constant and not to be affected by the actual corresponding VMA or SP dosages in the mixture. The saturation dosage of SP was also discussed in [53] with Marsh cone flow tests. Results showed that the saturation dosage could increase with a reduction in W/B, additional mineral admixtures with higher water demand, or increase in silica fume etc., and the dosage could vary among different SP products.

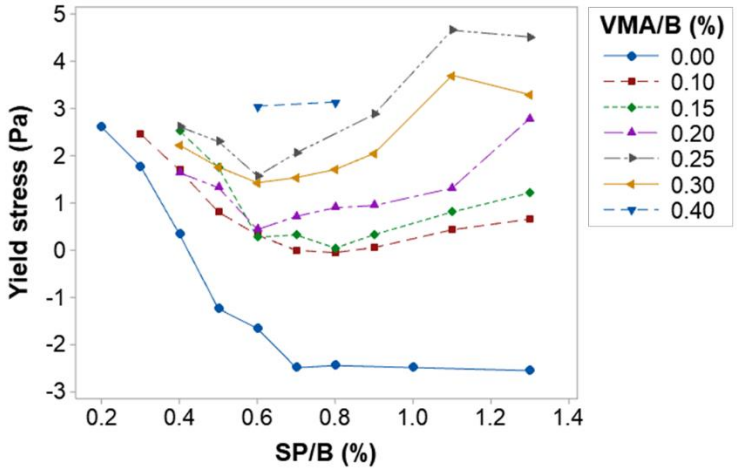

(a)

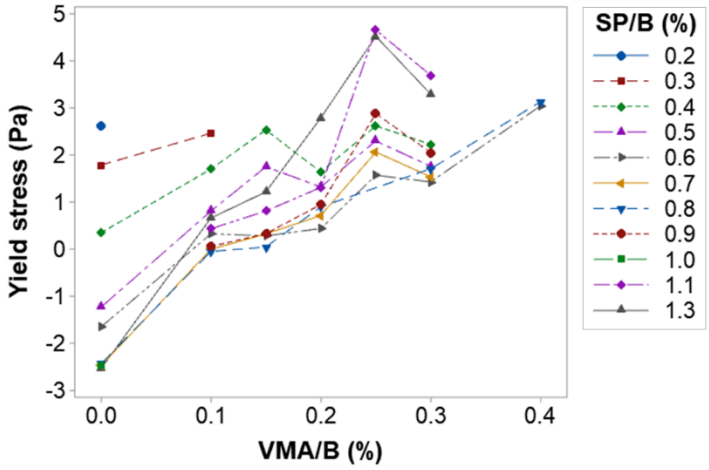

(b)

Fig. 6. Scatterplots of YS based on testing data vs (a) SP/B and (b) VMA/B.

3.1.2. Trends of PV with SP-VMA combinations

As shown in Fig. 7a, without VMA additions, PV steadily dropped with the increase of SP dosages, which was unfavourable for fibre dispersion and the mix would be prone to segregation. The PV as low as 0.8 Pa s was corresponding to the segregation status when YS started to be negative. In contrast, with VMA/B ≥ 0.10%, PV first increased and then levelled out (> 1.1 Pa s) with increasing SP, thus avoiding segregation. The high PV could aid efficient fibre dispersion. As shown in Fig. 7b, when the VMA dosage increased from 0.10%

to 0.40%, PV only slightly increased, indicating that high dosage of VMA was not efficient at increasing PV unlimitedly.

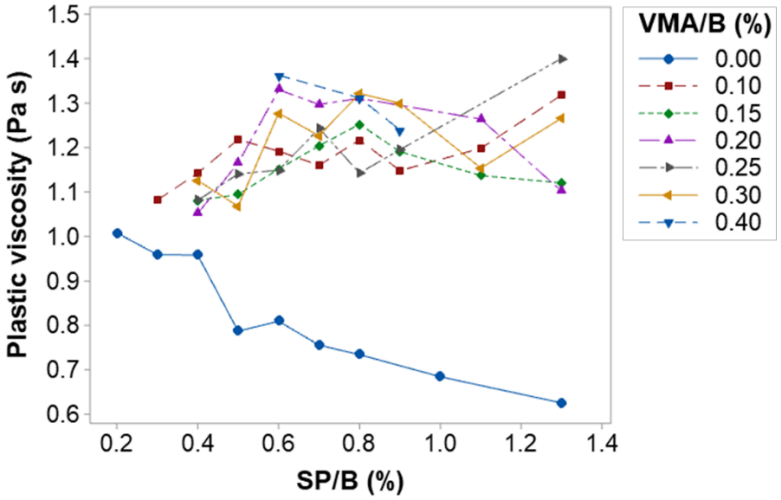

(a)

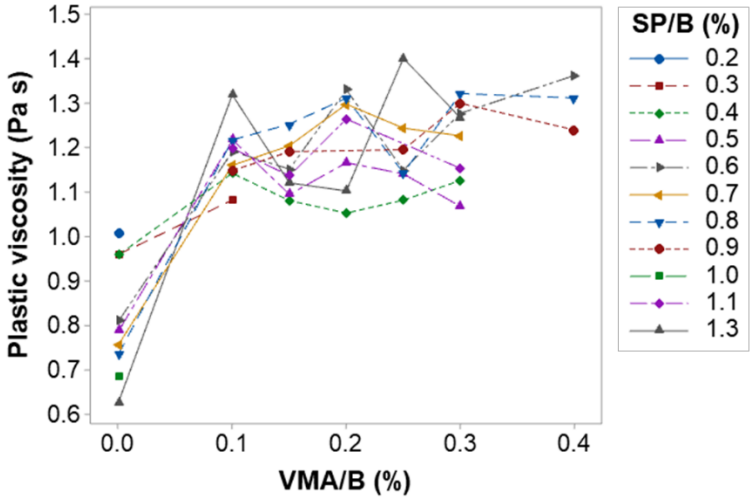

(b)

Fig. 7. Scatterplots of PV based on testing data vs (a) SP/B and (b) VMA/B.

3.2. Regression analysis, modelling and prediction

Although testing data could indicate the general trends of YS and PV with SP-VMA dosages, those could be subjected to various errors and could not be directly used for further prediction of rheological behaviour with other SP-VMA dosages. Therefore, regression analysis was conducted to generalise the patterns. In this study, the two variables, *SP/B* and *VMA/B* were entered as designed predictors, and the test data of YS and PV were fitted separately to obtain the 2-variable surface models for each response variable. 40 sets of SP-VMA combinations were used for modelling and another 10 sets within the same range were used for prediction validation and model evaluation.

The commercial statistical software Minitab [54] was used for regression analysis. Two basic statistics were applied for evaluating the quality of regression. R-squared (R^2) could show how well the model fits the data; the higher of which indicates better fitting (maximum 100%). The standard error (SE) means the average distance between the regression surface and the surface of directly tested data. There are three types of R^2 for evaluating the modelling results. The basic R^2 can always be increased when more terms are incorporated in the model, not

necessarily increasing the modelling and prediction efficiency. So the adjusted R^2 considers the number of predictors, suitable for comparing models with different numbers of predictors. Predicted R^2 is more representative to evaluate the predictive ability of the model for new observations. Therefore, the optimal models in this study were tuned and determined to achieve the highest predicted R^2 to balance between the model complexity, efficiency and predictive ability. Besides, the analysis of variance (ANOVA) was applied to evaluate the significance of each terms in the models. A p-value smaller than 0.05 means the term is significant.

The fitting process started from simple linear and was gradually added on with higher-order terms and interaction terms based on the fitting quality to better describe the nonlinear curvature trends. The predicted response is calculated as the sum of each term multiplied by their coefficient (Coef). Initially, hierarchical models were set up with the potential terms including 1) polynomial terms e.g. SP/B, $(SP/B)^2$, $(SP/B)^3$, VMA/B, $(VMA/B)^2$, $(VMA/B)^3$…, denoted as S1, S2, S3, V1, V2, V3… respectively; 2) interaction terms e.g. (SP/B)*(VMA/B), $(SP/B)^2$* (VMA/B), (SP/B)*$(VMA/B)^2$…, denoted as S1V1, S2V1, S1V2… respectively. The unit for S1 and V1 was %. Based on fitting results and model optimisation, statistically insignificant terms (with $p \geq 0.05$) were replaced or removed from the models and eventually highest predicted R^2 were achieved to maintain a high predictive ability of the models.

3.2.1. Modelling of yield stress (YS)

As shown in Table 4, five significant terms (corresponding to five degrees of freedom (DF) with p-values less than 0.05) were involved in the model for fitting the YS testing data. The corresponding R^2 was 91.55%, adjusted R^2 was 90.34% and predicted R^2 was 87.89%. The three values were all close to 1 and also close to each other, showing that the model fitted the testing data well and the model was not overfitted. Based on the degree of contribution (ρ%), SP showed a larger effect on the variation of YS than VMA (which was mainly reduction effect since the coefficient of S2 was negative). The interaction term S1V1 also had a large contribution (32.51%), confirming that SP and VMA had a significant interactive effect with each other on YS and VMA mainly contributed to the YS increase.

Table 4. Model summary and analysis of variance for the response YS.

Terms	Coef	SE Coef	T-Value	DF	Adj SS	Adj MS	F-Value	p-value	Sig	ρ%
Constant	4.132	0.471	8.77							
S2	-42.58	5.34	-7.97	1	20.567	20.5672	63.58	<0.0001	Y	28.86
S1V1	25.84	3.05	8.46	1	23.166	23.1664	71.62	<0.0001	Y	32.51
S3	57.83	8.74	6.62	1	14.164	14.1639	43.79	<0.0001	Y	19.88
S1V2	-24.49	8.55	-2.86	1	2.652	2.6517	8.2	0.007	Y	3.72
S4	-21.69	3.77	-5.75	1	10.7	10.7005	33.08	<0.0001	Y	15.02
Error				35	11.322	0.3235				
Total				40	134.012					

(*Coef: coefficient for each term; SE Coef: standard error for each coefficient; Adj: adjusted; Pred: predicted; DF: degree of freedom; SS: sum of squares; MS: mean square; Sig: significancy; Y: yes; ρ%: degree of contribution = individual F-value/sum of F-values)

Comparing Fig. 8a with Fig. 8b, the model could estimate well the YS zone between 0.5 Pa and 1.5 Pa. The model seemed to slightly overestimate the area of segregation zone (YS < 0 Pa) and also overestimated high YS values (> 2 Pa). However, the former would contribute to a more conservative estimation of the ideal area in between (with relatively low but still positive YS), and the latter (high YS zone) would normally not be of interest. The 3-D surface plot is in presented in Fig. 9.

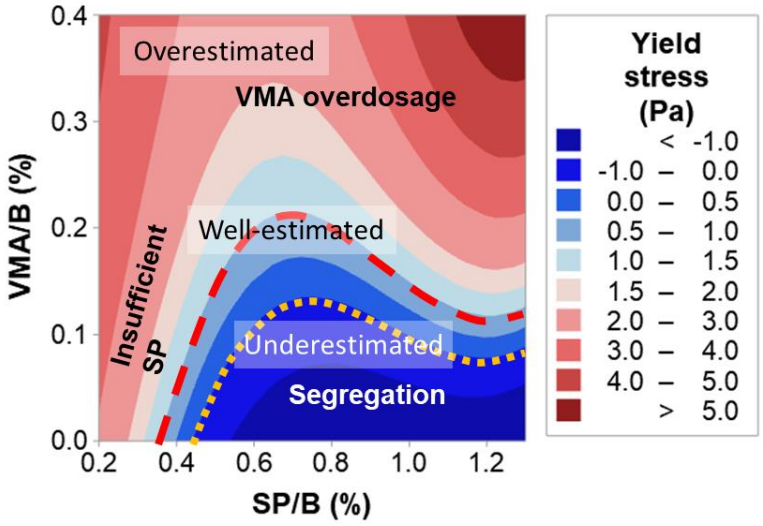

(a)

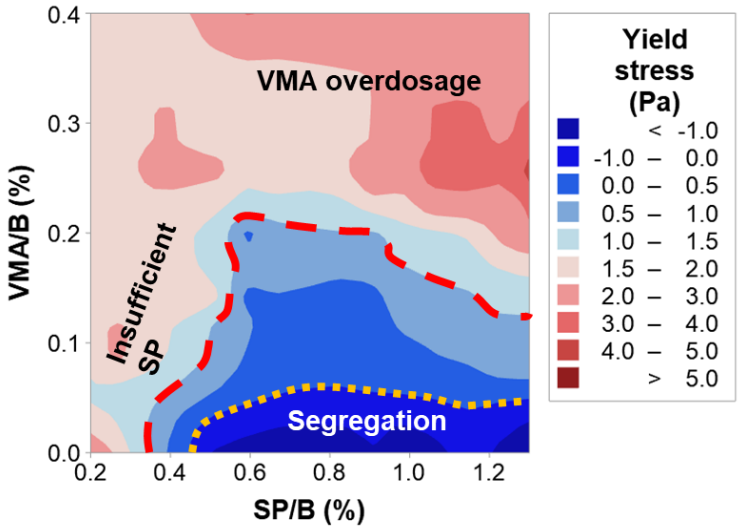

(b)

Fig. 8. Contour maps of YS with SP/B and VMA/B: (a) modelling results (b) data from rheology tests. The red dash line is the contour for 1.0 Pa and the yellow dash lines are the contours for 0 Pa (below which is segregation area).

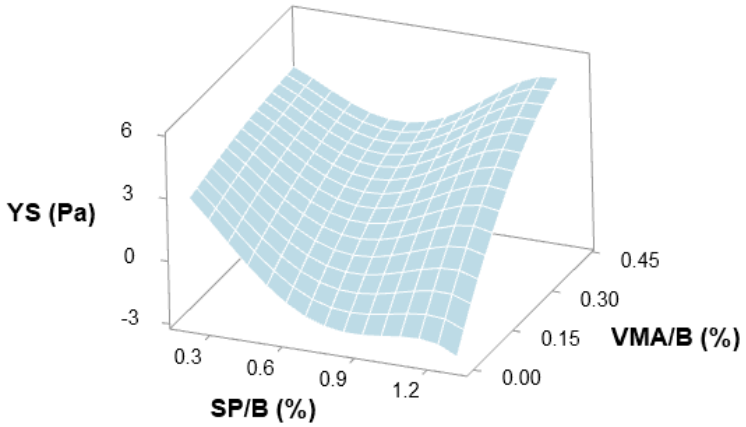

Fig. 9. 3-D surface plot of YS with SP/B and VMA/B based on regression analysis.

3.2.2. Modelling of plastic viscosity (PV)

Seven statistically significant terms (i.e. seven DF) were involved in the PV model for achieving the highest predicted R^2 (provided in Table 5). The resulting R^2 was 85.66%, adjusted R^2 was 82.62% and predicted R^2 was 76.23%. The fitting performance was not as high as that for YS, which was because many PV data was close to each other and the changing trend was not apparent. But the model still provided a good guidance regarding how to increase PV and avoid segregation by adjusting SP-VMA dosages, and what the saturation dosages of VMA was (as shown in Fig. 10a). Based on ρ%, the individual terms (S2, V2, S3, V3) showed similar percent contribution with the interaction terms (S1V1, S2V1, S1V2), i.e. around 50% for each group, and the coefficients included both positive and negative values, indicating that the change of PV was highly dependent on both SP and VMA dosages with interacting and competing effects in between. VMA had a larger effect on the variation of PV than SP according to both the percent contribution and the contour maps in Fig. 10.

Table 5. Model summary and analysis of variance for the response PV.

Terms	Coef	SE Coef	T-Value	DF	Adj SS	Adj MS	F-Value	p-value	Sig	ρ%
Constant	1.0105	0.045	22.45							
S2	-0.777	0.238	-3.26	1	0.0675	0.0675	10.63	0.003	Y	8.37
V2	-14.21	3.32	-4.28	1	0.1166	0.1166	18.36	<0.0001	Y	14.46
S1V1	9.96	1.44	6.9	1	0.3024	0.3024	47.62	<0.0001	Y	37.50
S3	0.432	0.181	2.39	1	0.0361	0.0361	5.69	0.023	Y	4.48
V3	30.57	6.56	4.66	1	0.1378	0.1378	21.71	<0.0001	Y	17.09
S2V1	-2.97	1.12	-2.66	1	0.0449	0.0449	7.07	0.012	Y	5.57
S1V2	-11.86	2.97	-3.99	1	0.1011	0.1011	15.92	<0.0001	Y	12.54
Error				33	0.2096	0.0064				
Total				40	1.4613					

As shown in Fig. 10a and Fig. 10b, higher PV values above 1.15 Pa s were fitted well by the model, which would be the targeted PV area. Although the model underestimated the PV values when the VMA was overdosed (> 0.20%) and SP was lacking (< 0.40%) (i.e. stiff mixtures), it would still contribute to a safer estimation. The 3-D surface plot of PV model is provided in Fig. 11.

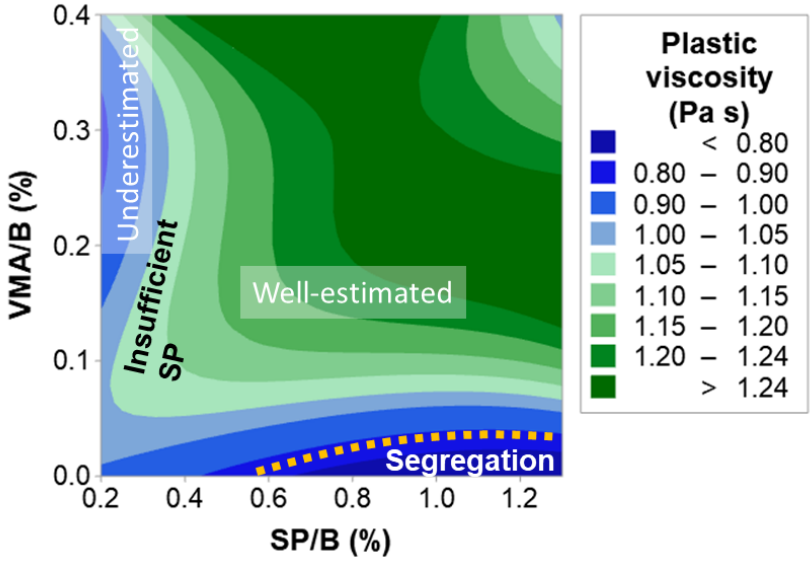

(a)

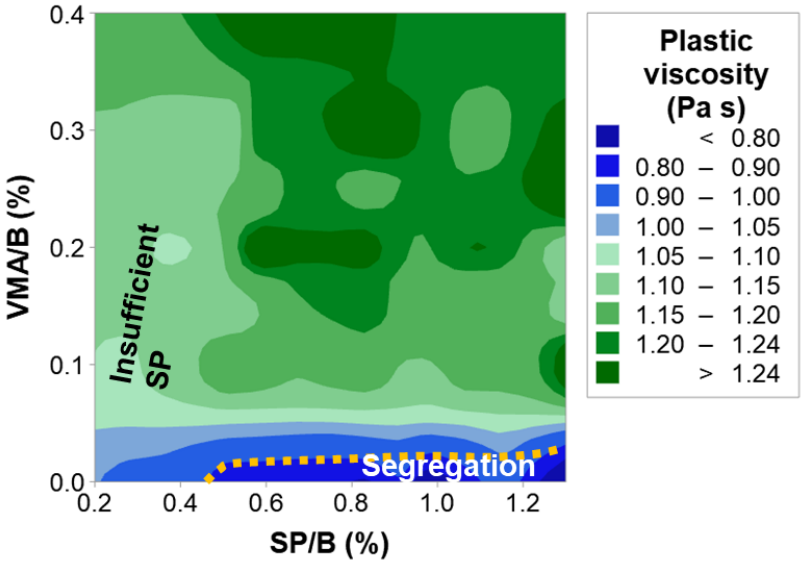

(b)

Fig. 10. Contours maps of PV with SP/B and VMA/B: (a) modelling results (b) data from rheology tests. The yellow dash lines are the boundaries for segregation area.

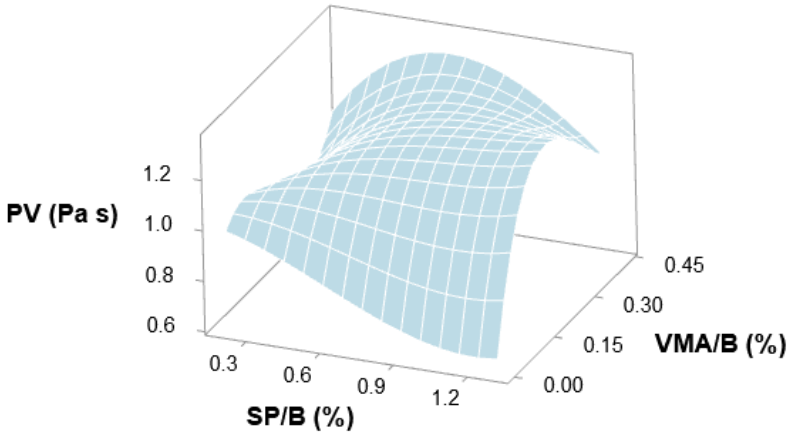

Fig. 11. 3-D surface plot of PV with SP/B and VMA/B based on regression analysis.

3.2.3. Prediction practice and model validation

Since 40 data sets with different SP-VMA combinations were applied in fitting, additional 10 sets of combinations were input in the models for prediction of YS and PV and model validation. The 10 sets were also tested in rheology tests to compare with the predicted values and evaluate the modelling quality. Results are shown in Fig. 12. The x-axis represents the measured values with standard deviations, and the y-axis shows the predicted values with standard deviations. Most of the data points with their variance ranges successfully covered the y = x reference line, indicating acceptable errors and satisfying prediction.

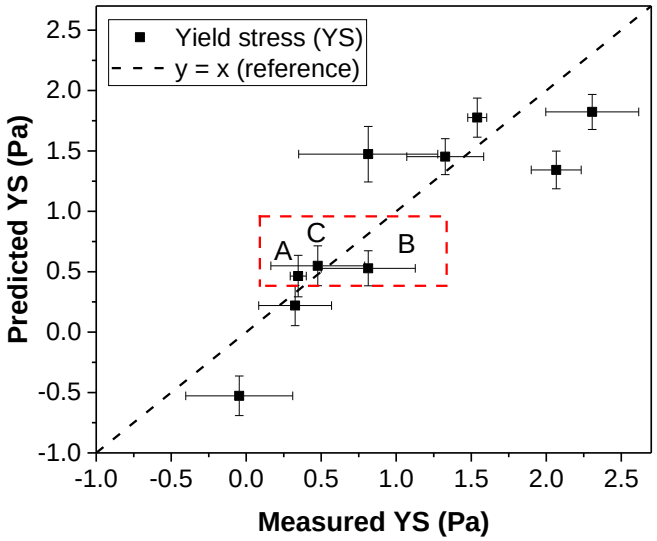

(a)

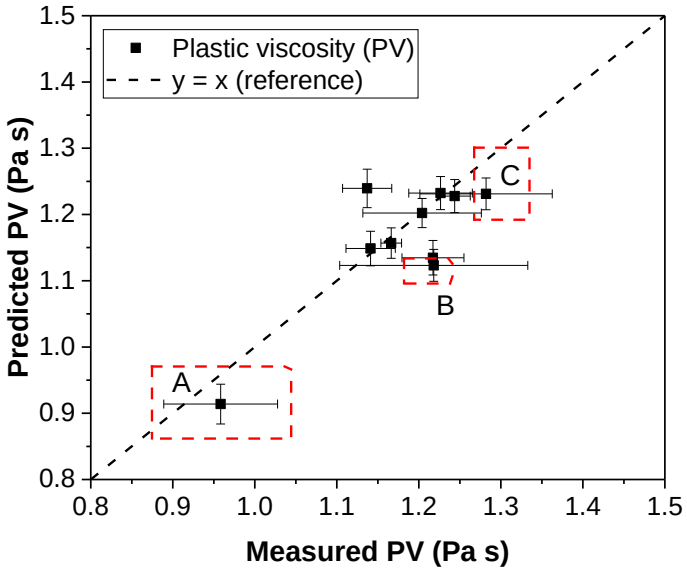

(b)

Fig. 12. Comparison of (a) predicted YS vs measured YS (b) predicted PV vs measured PV based on different SP-VMA combinations. The three rheology conditions A, B, C are corresponding to the three ECC batches for mechanical testing with similar YS but different PV.

3.2.4. Method for SP-VMA design

If the two contour maps are overlapped, then the rheological response of different SP-VMA combinations could be predicted, and the objective range of SP-VMA combinations (or target zone in the SP-VMA map) for optimal rheology could be determined depending on specified requirements (Fig. 13). Firstly, YS should be as low as possible to ensure flowability but should not be below zero, i.e. the region should be between the red curve (maximum workable YS) and the orange curve (segregation threshold). Secondly, high enough PV should be achieved. And the maximum allowable YS and minimum PV required should be dependent on the fibre, matrix and interfacial properties and could be confirmed in practice. The recommended YS based on mixing and casting experience in this study is around 0.5 Pa and should not exceed 1.0 Pa. This range has been reasonably agreed by [30] based on both

modelling and experimental results. Accordingly, since too high VMA dosage would cause an increase in YS as discussed before, the VMA dosage should be set between 0.10% and 0.20%. Contour lines could be referred for designing for different PV (e.g. the yellow and white curves in Fig. 13). As long as the SP-VMA combinations are within the designed range, satisfying and uniform fibre dispersion should be realised, and a stable and cohesive ECC mixture could be produced. It could be noticed that without VMA, the range of SP dosage for appropriate YS was very limited (spot A in Fig. 13), and the overdosage of SP would easily lead the rheology behaviour to the segregation area; with VMA addition, the range of applicable SP dosage became wider, so the mixture would be less prone to segregation.

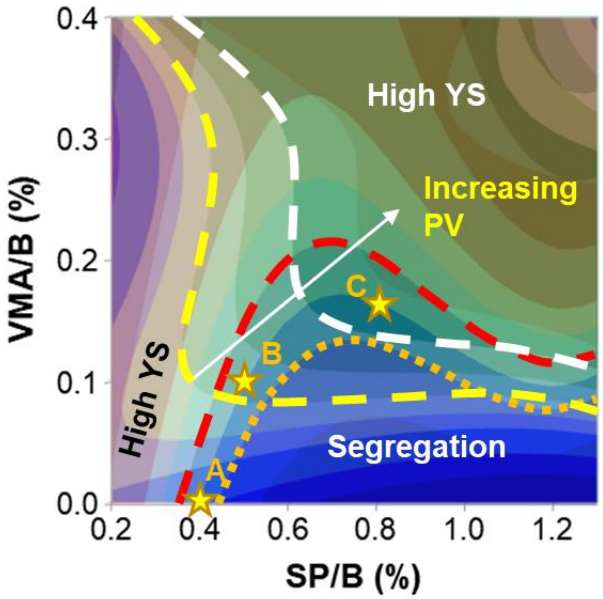

Fig. 13. Strategy for determining SP-VMA dosages for ECC mixing by overlapping YS and PV contour plots. The dash lines represent different contour lines. The red line is a YS contour line, representing the maximum allowable YS based on experience (YS = 1.0 Pa in this study); the orange one is the YS contour line as the boundary of the segregation area; the yellow one is the PV contour line representing PV = 1.10 Pa s; the white one is the PV contour line of PV = 1.20 Pa s. The three star signs represent three SP-VMA combinations for model validation through mechanical testing, which could result in similar YS but varying PV, potentially leading to different mechanical behaviour of hardened ECC specimens.

3.3. Further method validation through flexural tests

In order to compare the mechanical performance (affected by fibre distribution) of hardened specimens produced with different fresh rheology conditions, three SP-VMA combinations were selected and applied for batch mixing (all marked with star signs in Fig. 13). Specifically, as predicted in Fig. 12, Combination A (0.40% SP), Combination B (0.50% SP + 0.10% VMA) and Combination C (0.80% SP+ 0.17% VMA) had similar YS around 0.5 Pa but varying PV. The YS was confirmed to achieve sufficient flowability for adding fibres and successful specimen casting without causing major defects or segregation. Combination A was predicted to have the lowest PV since no VMA was added, which might result in insufficient fibre dispersion, thus leading to inefficient fibre bridging and low ductility; Combination C was expected to achieve the highest PV with the help of VMA, which could potentially contribute to more uniform fibre mixing and higher ductility. Accordingly, three batches of ECC with these SP-VMA combinations were mixed and casted for curing until 28 days. During mixing, the similar YS for different batches was verified by flow table tests, showing similar flow spread of 280±10 mm. The hardened specimens were then loaded in four-point flexural tests to verify the validity and efficiency of the modelling and prediction. The average modulus of rupture (MOR) and flexural deflection capacity for each batch could

indicate fibre bridging capacity, which was affected by the extent of fibre dispersion and fibre-matrix interfacial properties.

Fig. 14 shows representative flexural stress-midspan deflection curves of the 28-d specimens from the three batches based on different SP-VMA combinations. Fig. 15 presents the main flexural properties. The matrix properties, mainly the flaw size distribution and matrix fracture toughness, could be indirectly indicated by the first cracking strength and also elastic stiffness (Fig. 15a). The similar first cracking strength and elastic modulus among the three ECCs could indicate similar matrix properties and negligible effects on matrix properties brought by the varying admixture dosages in this study. Combination A led to relatively low ductility and MOR of the corresponding hardened specimens (Fig. 15b), i.e. the full potential for strain-hardening, multiple cracking and MOR development was hindered by the weak sections in the specimens, indicating that the fresh viscosity was not enough for uniform and sufficient fibre dispersion. Combination B and C both resulted in similarly high deflection capacity and high MOR with tolerable variance, indicating that the fibre distribution was satisfying and the rheology was appropriate. Comparing Combination B and C with Combination A (with similar YS but lower PV), the deflection capacity was improved by 200%. Furthermore, the PV due to Combination B was already sufficient for uniform fibre mixing, so even higher PV (as for Combination C) did not add on any further benefits; this is agreed by [22]. To conclude, the flexural performance (especially deflection capacity) of hardened ECC was consistent with the predicted rheology based on regression analysis, further supporting the modelling results and the method for rheology design.

Additionally, it could be noticed that the variability of deflection capacity among the three combinations was much higher than that of MOR, and this was due to the nature of the mix design. According to micromechanics, the variability of deflection capacity, or the robustness of ductility, depends on the difference between matrix cracking strength and fibre bridging strength, i.e. PSH_strength, and also between the crack tip toughness and complimentary energy, i.e. PSH_energy [55]. It has been advised that PSH_energy should be larger than 3 for robust strain-hardening. When the PSH parameters are low due to the nature of mix design and the reduced fibre bridging capacity, the deflection capacity can be highly variable. This indicates that moderate reduction of fibre bridging strength because of insufficient fibre distribution (represented by MOR in bending tests) could result in a massive reduction in deflection capacity if the first cracking strength is very close to MOR, which is why the difference in deflection capacity was this significant in our study. This result also emphasizes the importance of uniform fibre distribution for maximising fibre bridging efficiency, minimising variability and improving the robustness of strain-hardening property.

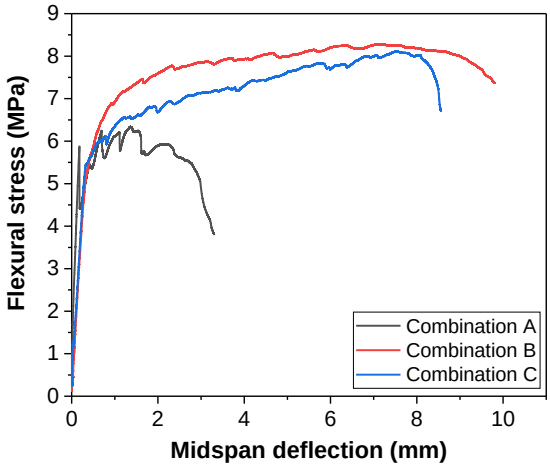

Fig. 14. Typical flexural stress-deflection curves of 28-d ECC with different SP-VMA dosage combinations.

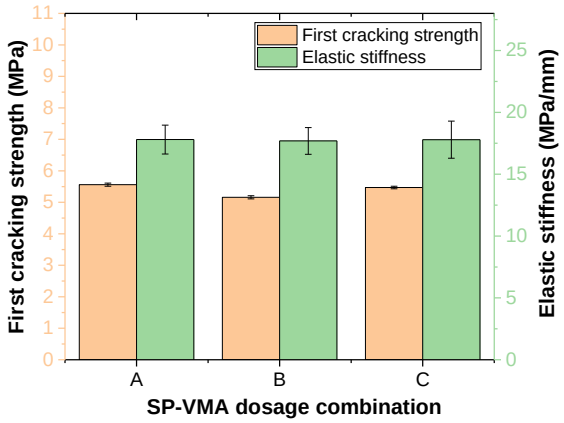

(a)

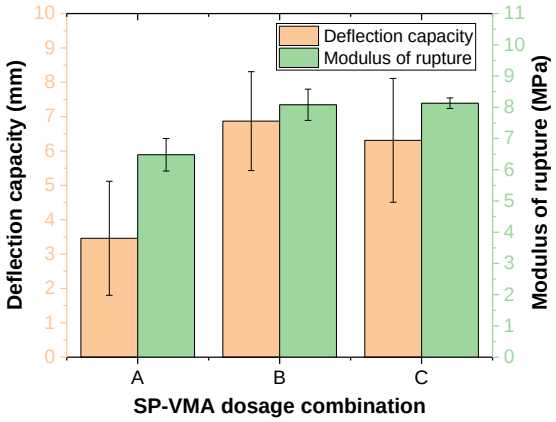

(b)

Fig. 15. Flexural properties of 28-d ECC with different SP-VMA dosage combinations (a) Matrix properties; (b) properties indicating fibre bridging.

3.4. Hydration rate, setting time & compressive strength development

To further investigate the influence of different SP-VMA additions on the hydration process, the two SP-VMA combinations with appropriate rheology and satisfying flexural performance, B and C, were investigated regarding their effects on hydration rate and heat release. As shown in Fig. 16, more SP and VMA addition would mainly slow down the hydration process, i.e. it delayed the power peaks, reduced the peak values, and also reduced the total energy release until 100 hrs. High dosages of SP and VMA could delay the setting time to even 2.5 days.

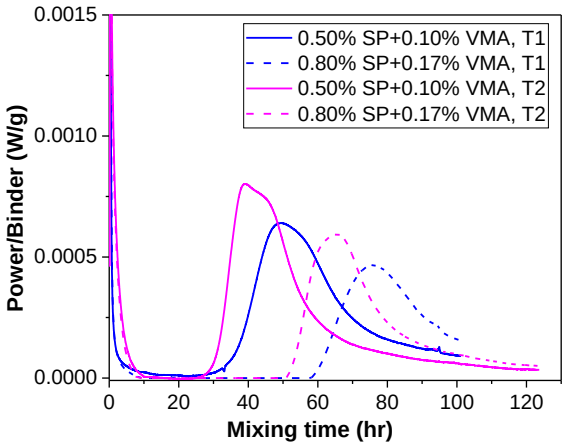

(a)

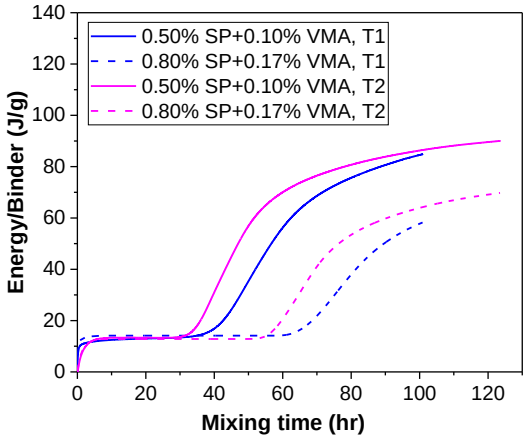

(b)

Fig. 16. (a) Unit power and (b) hydration heat of F28-ECC mortar with different SP-VMA combinations (T1, T2 represent testing replicates).

Considering the cumulative energy curves had not level out until 100 hrs after mixing, the early-age compressive strength development with different SP-VMA dosages was tested. The 3-d compressive strength was 16.34 (±1.18) MPa for Combination B but only 10.05 (±0.74) MPa for Combination C, which conformed to the 72-hr hydration heat; while the 7-d compressive strength for the two batches was comparable, which was 22.63 (±1.02) MPa for Combination B and 22.97 (±0.63) MPa for Combination C. This indicates that the different dosages of SP and VMA could slow down the strength development to different extent at early age (mainly before 7 days). Therefore, too high dosages of SP and VMA could be undesirable for the real application conditions, especially for mixes already having a large proportion of SCMs. Additionally, the small variance of compressive strength among samples could indicate satisfying matrix consistency of both batches.

3.5. General guidelines for applying admixtures for rheology control of ECC mortar

The general effects of SP and VMA on the rheological properties of ECC based on the testing data in this study can be summarised in Fig. 17.

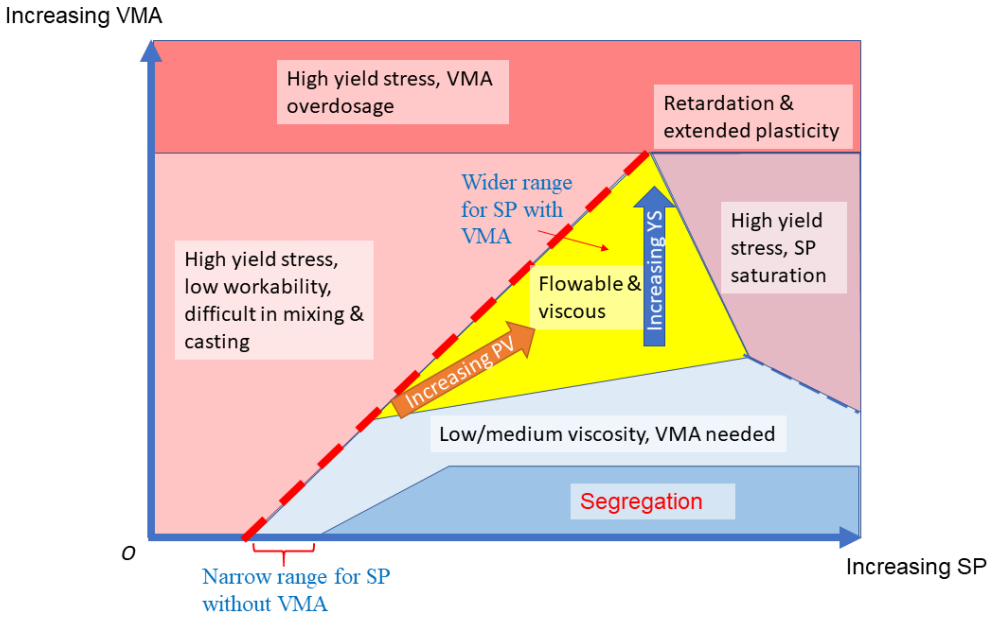

Fig. 17. General effects of SP and VMA on ECC for rheology design. Different locations on the plane represent different SP-VMA combinations, corresponding to varying rheological conditions. The flowable and viscous region (highlighted in bright yellow) is the appropriate design zone for ECC.

When VMA is not incorporated (i.e. horizontal axis in Fig. 17), insufficient SP dosage would lead to a stiff mixture, while overdosed SP will cause irreversible segregation and should be avoided. Therefore, there could be a range of SP dosage for achieving enough fluidity without segregation. Whether VMA is necessary to work together with SP for uniform fibre mixing and stability of ECC depends on how wide the SP range is and what maximum viscosity could be generated in this SP range, which are governed by inherent/natural mixture cohesiveness and proneness to segregation. For example, coarser aggregates tend to reduce cohesion and could promote segregation; Class C fly ash with finer sphere-shaped particles and higher reactivity could generate higher frictional bonding than Class F fly ash, leading to higher viscosity [29]; longer fibres could bridge cracks more efficiently but could be harder to disperse and may cause segregation [24]. In occasions when a mixture is inherently prone to segregation, or the maximum viscosity is insufficient for satisfying fibre dispersion, VMA would be necessary and effective in preventing segregation, maintaining stability and improving fibre dispersion, as agreed by [29].

When appropriate dosage of VMA (e.g. 0.10 – 0.20% recommended in this study) is added, a wide range of SP-VMA combinations could effectively achieve the desired fresh status, i.e. with low yield stress and high flowability, and with sufficient viscosity to ensure uniform mixing and fibre distribution without segregation (yellow region in Fig. 17). On the other hand, slight overdosage of SP (with VMA incorporation) or VMA could still cause low viscosity or high yield stress (out of yellow region in Fig. 17), but since the mixture would be less prone to segregation, we could still take measures to remedy the fibre mixing, which is the added benefit of VMA. Specifically, if YS is too high with a high PV (stiff mix), higher mixing speed can be applied for generating higher shear stress to disperse the fibres; if YS is medium but PV is too low (close to segregation), longer mixing time could be applied to modify fibre distribution (since higher mixing speed with too high shear stress could still cause segregation). Finally, the effect of these admixtures on the hydration of the ECC should also be considered before an optimum combination is defined, because high dosages of SP and VMA could retard setting significantly and slow down the strength development.

4. Conclusions

In this study, the influence of SP and VMA dosage combinations on the rheological properties of high FA ECC mortar was systematically investigated and characterised in detail for the first time. Regression analysis was performed to generalise the rheology behaviour and for prediction. The optimal range of SP and VMA dosages for efficient mixing and fibre dispersion was effectively identified by the validated models and overlapping method. The method was further verified by mechanical testing. Based on the results, the following conclusions can be drawn:

(1) Based on Bingham model and rheology testing results, without VMA incorporation, increasing SP dosages rapidly reduced YS and also steadily reduced PV, when YS was below zero and PV was less than 0.8 Pa s, the mixture lost cohesiveness and segregation occurred. The segregation dosage of SP without VMA for this mixture was about 0.45%. On the other hand, with appropriate VMA addition, increasing SP dosages could still effectively reduce YS while maintaining PV above 1.1 Pa s. Therefore, segregation could be delayed or avoided, and high PV could also contribute to efficient fibre dispersion. Overdosage of VMA would not lead to even higher PV but could result in constantly high YS, which would increase difficulty in mixing and casting. The saturation dosages for both SP and VMA seemed to be constant (around 0.70% and 0.25% respectively) and not to be affected by the actual SP or VMA dosages in the mixture.

(2) Nonlinear polynomial regression modelling could effectively generalise and predict the rheology behaviour within the investigated scope (with R^2 around 90% for YS and 80% for PV). Due to the interactive effects of SP and VMA, a range of appropriate SP-VMA combinations for achieving ideal rheology for fibre distribution existed and could be effectively identified by the regression models and the overlapping method, hence the traditional trial-and-error and non-quantitative method for adding admixtures during batch mixing could be avoided.

(3) The importance of sufficient PV in addition to low YS during mixing was confirmed by bending tests, and the necessity of using VMA for fibre dispersion in mixtures with inherent low cohesiveness was highlighted. With appropriate SP-VMA combinations for achieving both sufficient PV and low YS, deflection capacity could be improved by 200%. Additionally, PV only needed to be sufficient for fibre dispersion, so higher PV did not add on further benefits for improving ductility.

(4) Depending on specific SP and VMA compositions, high dosages of these admixtures could decrease hydration rate and retard setting. The early-age strength development could be massively delayed, which could be unfavourable in specific field applications. According to mixing experience, when the mixture is not prone to segregation due to the stabilising effect of VMA, remedy measures could be taken to enhance fibre dispersion if the rheology is not optimum. Longer mixing time with medium speed is recommended when the viscosity is low and the mixture is too flowable, and higher mixing speed could be applied when the mixture is too stiff and not flowable enough.

(5) The aim of this study was to discern for the first time the combined effects of different dosages of SP and VMA on ECC mortar. Rheology trends and detailed patterns were obtained (characterised by YS and PV). Regression analysis was applied to establish and model the rheological behaviour for further prediction and deciding optimal SP-VMA dosages for ECC mixes. Results show that the proposed rheological trends and patterns and regression model formats are applicable for different occasions. Although the absolute values of YS and PV obtained from rheology tests, or the parameter values in models based on regression analysis could be different given different mixture characteristics, shearing profiles or temperature etc., the proposed method and modelling process could be further translated to other ECC materials with different local ingredient properties and mix proportions for precise rheology control. Moreover, for a specific type of fibre and fixed fibre content, the PV and YS required for uniform fibre distribution and sufficient workability can serve as a general reference; for the 2 vol% PVA fibres with oil

coating in this study, PV > 1.1 Pa s and 0.5 Pa < YS < 1 Pa is sufficient for achieving appropriate workability, cohesiveness and sufficient fibre dispersion. The proposed modelling and optimisation technique is a first step to providing a basis and practical guidance for applying combined chemical additives for rheology control, which would promote the extended adoption of ECC in engineering applications. For future work, analytical models could be developed to further consider the functioning mechanisms of these admixtures understanding better the effects and generalising the rheology behaviour for different mix design and testing parameters.

Acknowledgements

The financial support from the EPSRC for the Resilient Materials for Life (RM4L) Programme Grant (EP/P02081X/1) and the Cambridge Commonwealth, European and International Trust (CCEIT) for the first author's PhD research is gratefully acknowledged.

Reference

[1] V.C. Li, From micromechanics to structural engineering - the design of cementitious composites for civil engineering applications, J. Struct. Mech. Earthq. Eng. 10 (1993) 37–48.

[2] V.C. Li, On Engineered Cementitious Composites (ECC) - a review of the material and its applications, J. Adv. Concr. Technol. 1 (2003) 215–230. https://doi.org/10.3151/jact.1.215.

[3] K. Yu, L. Li, J. Yu, Y. Wang, J. Ye, Q. Xu, Direct tensile properties of engineered cementitious composites: A review, Constr. Build. Mater. 165 (2018) 346–362. https://doi.org/10.1016/j.conbuildmat.2017.12.124.

[4] G.J. Parra-Montesinos, High-performance fiber-reinforced cement composites: An alternative for seismic design of structures, ACI Struct. J. 102 (2005) 668–675.

[5] V.C. Li, T. Kanda, Innovations forum: Engineered Cementitious Composites for structural applications, J. Mater. Civ. Eng. 10 (1998) 66–69. https://doi.org/10.1061/(ASCE)0899-1561(1997)9:1(1).

[6] M.D. Lepech, V.C. Li, Long term durability performance of Engineered Cementitious Composites, Restor. Build. Monum. 12 (2006) 119–132. https://doi.org/https://doi.org/10.1515/rbm-2006-6038.

[7] S.F.U. Ahmed, H. Mihashi, A review on durability properties of strain hardening fibre reinforced cementitious composites (SHFRCC), Cem. Concr. Compos. 29 (2007) 365–376. https://doi.org/10.1016/j.cemconcomp.2006.12.014.

[8] M. Wu, B. Johannesson, M. Geiker, A review: self-healing in cementitious materials and engineered cementitious composite as a self-healing material, Constr. Build. Mater. 28 (2012) 571–583. https://doi.org/10.1016/j.conbuildmat.2011.08.086.

[9] G. Yildirim, Ö.K. Keskin, S.B.I. Keskin, M. Şahmaran, M. Lachemi, A review of intrinsic self-healing capability of engineered cementitious composites: recovery of transport and mechanical properties, Constr. Build. Mater. 101 (2015) 10–21. https://doi.org/10.1016/j.conbuildmat.2015.10.018.

[10] A. Zhao, J. Yang, E.H. Yang, Self-cleaning engineered cementitious composites, Cem. Concr. Compos. 64 (2015) 74–83. https://doi.org/10.1016/j.cemconcomp.2015.09.007.

[11] K.Q. Yu, J.T. Yu, J.G. Dai, Z.D. Lu, S.P. Shah, Development of ultra-high performance engineered cementitious composites using polyethylene (PE) fibers, Constr. Build. Mater. 158 (2018) 217–227. https://doi.org/10.1016/j.conbuildmat.2017.10.040.

[12] R. Ranade, V.C. Li, M.D. Stults, W.F. Heard, T.S. Rushing, Composite properties of high-strength, high-ductility concrete, ACI Mater. J. 110 (2013) 413–422. https://doi.org/10.3868/s110-003-014-0039-x.

[13] V.C. Li, Y.M. Lim, Y.W. Chan, Feasibility study of a passive smart self-healing

cementitious composite, Compos. Part B Eng. 29 (1998) 819–827. https://doi.org/10.1016/S1359-8368(98)00034-1.
[14] D. Snoeck, N. De Belie, Repeated autogenous healing in strain-hardening cementitious composites by using superabsorbent polymers, J. Mater. Civ. Eng. 28 (2016) 04015086-1–11. https://doi.org/10.1061/(ASCE)MT.1943-5533.
[15] H. Siad, M. Lachemi, M. Sahmaran, H.A. Mesbah, K.A. Hossain, Advanced engineered cementitious composites with combined self-sensing and self-healing functionalities, Constr. Build. Mater. 176 (2018) 313–322. https://doi.org/10.1016/j.conbuildmat.2018.05.026.
[16] V.C. Li, Engineered Cementitious Composites - Bendable concrete for sustainable and resilient infrastructure, Springer-Verlag, GmbH Germany, 2019. https://doi.org/10.1007/978-3-662-58438-5.
[17] V.C. Li, S. Wang, Microstructure variability and macroscopic composite properties of high performance fiber reinforced cementitious composites, Probabilistic Eng. Mech. 21 (2006) 201–206. https://doi.org/10.1016/j.probengmech.2005.10.008.
[18] K. Tosun-Felekoğlu, B. Felekoğlu, R. Ranade, B.Y. Lee, V.C. Li, The role of flaw size and fiber distribution on tensile ductility of PVA-ECC, Compos. Part B Eng. 56 (2014) 536–545. https://doi.org/10.1016/j.compositesb.2013.08.089.
[19] N. Ozyurt, T.O. Mason, S.P. Shah, Correlation of fiber dispersion, rheology and mechanical performance of FRCs, Cem. Concr. Compos. 29 (2007) 70–79. https://doi.org/10.1016/j.cemconcomp.2006.08.006.
[20] J.K. Kim, J.S. Kim, G.J. Ha, Y.Y. Kim, Tensile and fiber dispersion performance of ECC (engineered cementitious composites) produced with ground granulated blast furnace slag, Cem. Concr. Res. 37 (2007) 1096–1105. https://doi.org/10.1016/j.cemconres.2007.04.006.
[21] R. Ranade, M.D. Stults, B. Lee, V.C. Li, Effects of fiber dispersion and flaw size distribution on the composite properties of PVA-ECC, in: G.J. Parra-Montesinos, H.W. Reinhardt, A.E. Naaman (Eds.), High Perform. Fiber Reinf. Cem. Compos. 6 RILEM State Art Reports, Springer, Dordrecht, 2012: pp. 107–114. https://doi.org/10.1007/978-94-007-2436-5_14.
[22] M. Li, V.C. Li, Rheology, fiber dispersion, and robust properties of Engineered Cementitious Composites, Mater. Struct. 46 (2013) 405–420. https://doi.org/10.1617/s11527-012-9909-z.
[23] B.Y. Lee, J.K. Kim, J.S. Kim, Y.Y. Kim, Quantitative evaluation technique of Polyvinyl Alcohol (PVA) fiber dispersion in engineered cementitious composites, Cem. Concr. Compos. 31 (2009) 408–417. https://doi.org/10.1016/j.cemconcomp.2009.04.002.
[24] Y. Akkaya, S.P. Shah, B. Ankenman, Effect of fiber dispersion on multiple cracking of cement composites, J. Eng. Mech. 127 (2001) 311–316. https://doi.org/https://doi.org/10.1061/(ASCE)0733-9399(2001)127:4(311).
[25] S. Wang, V.C. Li, Tailoring of pre-existing flaws in ECC matrix for saturated strain hardening, in: Fract. Mech. Concr. Concr. Struct. Fram., 2004: pp. 1005–1012. https://deepblue.lib.umich.edu/bitstream/handle/2027.42/84774/WangFramcos5.pdf?sequence=1&isAllowed=y (accessed April 22, 2019).
[26] L. Ferrara, A. Meda, Relationships between fibre distribution, workability and the mechanical properties of SFRC applied to precast roof elements, Mater. Struct. 39 (2006) 411–420. https://doi.org/10.1617/s11527-005-9017-4.
[27] Y. Yang, Methods study on dispersion of fibers in CFRC, Cem. Concr. Res. 32 (2002) 747–750. https://doi.org/10.1016/S0008-8846(01)00759-1.
[28] B.M. Tyson, R.K. Abu Al-Rub, A. Yazdanbakhsh, Z. Grasley, A quantitative method for analyzing the dispersion and agglomeration of nano-particles in composite materials, Compos. Part B Eng. 42 (2011) 1395–1403. https://doi.org/10.1016/j.compositesb.2011.05.020.
[29] E.-H. Yang, M. Sahmaran, Y. Yang, V.C. Li, Rheological control in production of engineered cementitious composites, ACI Mater. J. 106 (2009) 357–366.

[30] M. Sahmaran, Z. Bilici, E. Ozbay, T.K. Erdem, H.E. Yucel, M. Lachemi, Improving the workability and rheological properties of Engineered Cementitious Composites using factorial experimental design, Compos. Part B. 45 (2013) 356–368. https://doi.org/10.1016/j.compositesb.2012.08.015.
[31] P.F.G. Banfill, Rheological methods for assessing the flow properties of mortar and related materials, Constr. Build. Mater. 8 (1994) 43–50. https://doi.org/10.1016/0950-0618(94)90007-8.
[32] R. Flatt, I. Schober, Superplasticizers and the rheology of concrete, in: Underst. Rheol. Concr., Woodhead Publishing Limited, 2012: pp. 144–208. https://doi.org/10.1016/B978-0-85709-028-7.50007-8.
[33] J. Zhou, S. Qian, G. Ye, O. Copuroglu, K. Van Breugel, V.C. Li, Improved fiber distribution and mechanical properties of engineered cementitious composites by adjusting the mixing sequence, Cem. Concr. Compos. 34 (2012) 342–348. https://doi.org/10.1016/j.cemconcomp.2011.11.019.
[34] M. Keskinateş, B. Felekoğlu, The influence of mineral additive type and water/binder ratio on matrix phase rheology and multiple cracking potential of HTPP-ECC, Constr. Build. Mater. 173 (2018) 508–519. https://doi.org/10.1016/j.conbuildmat.2018.04.038.
[35] F. Faroug, J. Szwabowski, S. Wild, Influence of superplasticizers on workability of concrete, J. Mater. Civ. Eng. 11 (1999) 151–157. https://doi.org/10.1061/(asce)0899-1561(1999)11:2(151).
[36] J. Gołaszewski, J. Szwabowski, Influence of superplasticizers on rheological behaviour of fresh cement mortars, Cem. Concr. Res. 34 (2004) 235–248. https://doi.org/10.1016/j.cemconres.2003.07.002.
[37] K.H. Khayat, Z. Guizani, Use of viscosity-modifying admixture to enhance stability of fluid concrete, ACI Mater. J. 94 (1997) 332–340. https://doi.org/10.14359/317.
[38] H.J. Kong, S.G. Bike, V.C. Li, Constitutive rheological control to develop a self-consolidating engineered cementitious composite reinforced with hydrophilic poly(vinyl alcohol) fibers, Cem. Concr. Compos. 25 (2003) 333–341. https://doi.org/10.1016/S0958-9465(02)00056-2.
[39] A. Leemann, F. Winnefeld, The effect of viscosity modifying agents on mortar and concrete, Cem. Concr. Compos. 29 (2007) 341–349. https://doi.org/10.1016/j.cemconcomp.2007.01.004.
[40] A. Yahia, K.H. Khayat, Experiment design to evaluate interaction of high-range water-reducer and antiwashout admixture in high-performance cement grout, Cem. Concr. Res. 31 (2001) 749–757. https://doi.org/10.1016/S0008-8846(01)00496-3.
[41] E.-H. Yang, Y. Yang, V.C. Li, Use of high volumes of fly ash to improve ECC mechanical properties and material greenness, ACI Mater. J. 104 (2007) 620–628. https://doi.org/10.14359/18966.
[42] Z. Zhang, S. Qian, H. Ma, Investigating mechanical properties and self-healing behavior of micro-cracked ECC with different volume of fly ash, Constr. Build. Mater. 52 (2014) 17–23. https://doi.org/10.1016/j.conbuildmat.2013.11.001.
[43] M. Şahmaran, V.C. Li, Durability properties of micro-cracked ECC containing high volumes fly ash, Cem. Concr. Res. 39 (2009) 1033–1043. https://doi.org/10.1016/j.cemconres.2009.07.009.
[44] M. Şahmaran, I.Ö. Yaman, M. Tokyay, Transport and mechanical properties of self consolidating concrete with high volume fly ash, Cem. Concr. Compos. 31 (2009) 99–106. https://doi.org/10.1016/j.cemconcomp.2008.12.003.
[45] E.-H. Yang, V.C. Li, Tailoring engineered cementitious composites for impact resistance, Cem. Concr. Res. 42 (2012) 1066–1071. https://doi.org/10.1016/j.cemconres.2012.04.006.
[46] K. Turk, M.L. Nehdi, Coupled effects of limestone powder and high-volume fly ash on mechanical properties of ECC, Constr. Build. Mater. 164 (2018) 185–192. https://doi.org/10.1016/j.conbuildmat.2017.12.186.
[47] C.F. Ferraris, K.H. Obla, R. Hill, The influence of mineral admixtures on the rheology of cement paste and concrete, Cem. Concr. Res. 31 (2001) 245–255.

https://doi.org/10.1016/S0008-8846(00)00454-3.
[48] British Standards Institution (BSI), BS EN 12350-5:2019. Testing fresh concrete Part 5: Flow table test, 2019.
[49] M. Maalej, V.C. Li, Flexural/tensile-strength ratio in engineered cementitious composites, J. Mater. Civ. Eng. 6 (1994) 513–528. https://doi.org/10.1061/(ASCE)0899-1561(1994)6:4(513).
[50] S. Qian, V.C. Li, Simplified inverse method for determining the tensile properties of strain hardening cementitious composites (SHCC), J. Adv. Concr. Technol. 6 (2008) 353–363. https://doi.org/10.3151/jact.6.353.
[51] ASTM, C1609/C1609M − 12 Standard test method for flexural performance of fiber-reinforced concrete (using beam with third-point loading), 2019. https://doi.org/10.1520/C1609_C1609M-12.
[52] British Standards Institution (BSI), BS EN 196-1:2016. Methods of testing cement Part 1: Determination of strength, 2016. https://doi.org/10.1590/S1413-294X2011000200001.
[53] L. Agulló, B. Toralles-Carbonari, R. Gettu, A. Aguado, Fluidity of cement pastes with mineral admixtures and superplasticizer—A study based on the Marsh cone test, Mater. Struct. 32 (1999) 479–485. https://doi.org/10.1007/bf02481631.
[54] Minitab 19 Statistical Software (2020). [Computer software]. University of Cambridge, England: Minitab, Inc. (www.minitab.com).
[55] V.C. Li, C. Wu, S. Wang, A. Ogawa, T. Saito, Interface tailoring for strain-hardening polyvinyl alcohol-engineered cementitious composite (PVA-ECC), ACI Mater. J. 99 (2002) 463–472. https://doi.org/10.14359/12325.